International Journal of Fracture, Vol. 15, No. 1, February 1979

Alphen aan den Rijn, The Netherlands

On the calibration of the electrical potential technique for monitoring crack growth using finite element methods

R.O. RITCHIE and K.J. BATHE

Department of Mechanical Engineering, Massachusetts Institute of Technology, Cambridge, Massachusetts, 02139, USA

(Received January 12, 1978; in revised form August 18, 1978)

ABSTRACT

Finite element analysis procedures are utilized to provide theoretical calibration curves for the electrical potential crack-monitoring system as applied to single-edge-notch (SEN) and compact tension (CT) fracture specimens. The results are compared to existing calibrations for such test piece geometries derived using experimental, electrical analog and analytical (conformal mapping) procedures.

1. Introduction

In recent years, much emphasis in fracture research has centered upon studies of the rate of propagation of sub-critical cracks. Accordingly, many experimental methods have been developed to monitor such crack growth. One of the most accurate and sensitive of these techniques currently in wide-spread use is the Electrical Potential Technique [1]. This method was first employed over thirty years ago for detecting surface cracks in large scale structures [2, 3]. In later years, electrical potential systems have been successfully applied to monitoring the propagation of fatigue [4], hydrogen embrittlement [5], stress corrosion [6], and creep [7] cracks, determining initiation of ductile crack growth in crack-opening displacement [8] and J_{Ic} [9] tests, measurement of velocities of fast running cleavage cracks [10], and assessing the proportion of crack closure in fatigue crack growth studies [11].

The basis of the method is that in a current carrying body there will be a disturbance in the electrical potential field about any discontinuity in that body. For the purposes of monitoring crack growth, the method entails passing a constant current (maintained constant by external means) through a cracked test specimen under load, and measuring the change in electrical potential across the crack. As this crack extends, the uncracked cross-sectional area of the test piece decreases, its electrical resistance increases, and thus the potential difference between two points on either side of the crack rises. By monitoring this potential increase (V_a), and comparing it with a reference potential (V_0) measured elsewhere on the test piece, preferably in a region unaffected by crack growth, the crack length (a) or crack length-to-specimen width ratio (a/W) may be determined, with the use of suitable calibration curves.

In practice, the accuracy of electrical potential measurements of crack length may be limited by a number of factors,* in particular by the determination of calibration curves relating changes in potential across the crack (V_a) to crack length (a). In most instances, experimental calibration curves have been obtained by

* Such factors include the electrical stability and resolution of the potential measurement system [23], electrical contact between crack surfaces where the fracture morphology is rough [22] or where significant crack closure effects are present [11], and changes in electrical resistivity with plastic deformation [23].

0376-9429/79/010047-09$00.20/0

measuring the electrical potential difference i) across machined slots of increasing length in a single test piece [23], ii) across a growing fatigue crack, where the length of the crack at each point of measurement is marked on the fracture surface by a single overload cycle or by a change in mean stress [2], or iii) across a growing fatigue crack in thin specimens where the length of the crack is measured by surface observation [13, 14]. Other experimental calibrations have been achieved using an electrical analog of the test piece [1], where the specimen design is duplicated, usually with increased dimensions for better accuracy, using graphitized analog paper [13] or thin aluminum foil [14], and where the crack length can be increased simply by cutting with a razor blade. Such calibration procedures, however, are relatively inaccurate, particularly at short crack lengths [15], and are tedious to perform. Furthermore, where measurements of crack initiation and early growth are required ahead of short cracks or notches or varying acuity, such procedures demand a new experimental calibration to be obtained for each notch geometry [14, 15].

Attempts at theoretical calibrations have involved finding solutions to Laplace's equation within the boundary conditions of a particular test piece geometry, where for a strip of metal, of constant thickness and width, containing a transverse crack, the steady electrical potential ϕ at a point (x, y) is given by

$$\nabla^2(\phi) = 0 \tag{1}$$

assuming that the current flows only in the plane of the strip (i.e. in the x-y plane). Analytical solutions to Eqn. (1) using conformal mapping techniques have been obtained for several simple geometries, namely center- and edge-cracked plates with razor slit starter notches [13, 17], and single-edge notched specimens with semi-elliptical, semi-circular and V-notches [15]. However, conformal mapping procedures are not easily applicable to more complex test piece geometries such as the widely used compact tension (CT) specimen. For such geometries, only experimental calibrations have been obtained, and consequently accurate measurements at short crack lengths become severely limited [15].

The object of the present work is to explore the feasibility of obtaining theoretical calibrations through the use of numerical solutions to (1) from finite element methods with the aim of providing a rapid and relatively inexpensive means of generating accurate calibrations for any required geometry. Solutions are obtained for the compact tension (CT) and single-edge-notch (SEN) test pieces and are compared with existing experimental calibrations for the CT test piece, and with experimental, electrical analog and analytical solutions for the SEN test piece.

2. Procedures

The test piece geometries considered, i.e. single-edge-notch (SEN) and compact tension (CT) specimens, are shown in Fig. 1. The SEN test-piece (Fig. 1a) is shown with a 45° V-notch, with the current introduced at the ends of the specimen (uniform current configuration). Potential changes (V_a) are measured from probes located 5.2 mm apart across the notch on the top surface of the specimen. The CT test piece (Fig. 1b) is shown in the standard 1-T ASTM configuration ($H/W = 0.6$), with the current introduced on the top surface (point application of current). Potential changes (V_a) are similarly measured from probes located 5.2 mm apart across the notch on the top surface. Based on electrical analog patterns, these locations of current input and potential measurement probes represent the optimum positions for these test piece geometries in terms of both sensitivity and reproducibility [1].

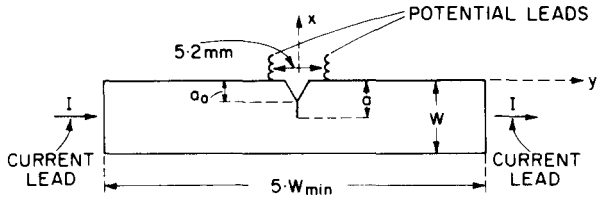

INITIAL CRACK LENGTH a_0= 5mm, WIDTH W=20mm

a) SINGLE-EDGED NOTCH (SEN) SPECIMEN - UNIFORM CURRENT CONFIGURATION

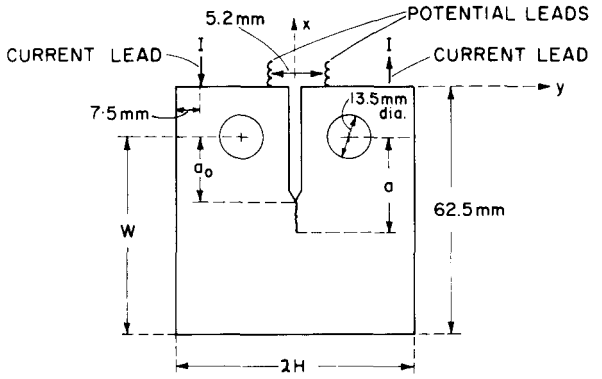

INITIAL CRACK LENGTH a_0 = 17.5mm, WIDTH W=50mm, 2H=60mm

b) COMPACT TENSION (CT) SPECIMEN - POINT APPLICATION OF CURRENT

Fig. 1. Test piece geometries investigated.

Experimental calibrations

Experimental calibrations for both geometries were determined by measuring the potential changes (V_a) in a single test piece where a crack length (a) was introduced by cutting 0.25 mm slots of increasing length at the bottom of the notch [23]. Measurements were taken with a constant stabilized DC current with the test piece at constant temperature (in melting ice at 0°C). The reference potential (V_{a0}) was measured across the initial notch ($a = a_0$) before cutting in the slots. Electrical analog calibrations for the SEN test piece were taken from the results of Clark and Knott [15] for an identical specimen geometry.

Finite element numerical calibrations

During recent years, the potential of the finite element method in the solution of general field problems has been recognized to an increasing extent [19, 20]. Assuming two-dimensional field conditions in the electric conduction problem of the test specimens considered here, the variational problem to be solved in the finite element solution is [19, 20],

$$\pi = \int_v 1/2k \left[\frac{\partial^2 \phi}{\partial x^2} + \frac{\partial^2 \phi}{\partial y^2}\right] dv - \int_{S_1} \phi^s i^s \, dS \tag{2}$$

$$\phi = \phi^s \text{ on } S_2 \tag{3}$$

with

$$\delta\pi = 0 \tag{4}$$

where k is the electric conductivity of the material, ϕ is the electric potential in the specimen and i^s is the boundary current specified on the surface S_1. The boundary conditions for the test specimen on surfaces S_1 and S_2 are shown in Figs. 2 and 3.

An effective finite element solution to the problem is obtained using variable-

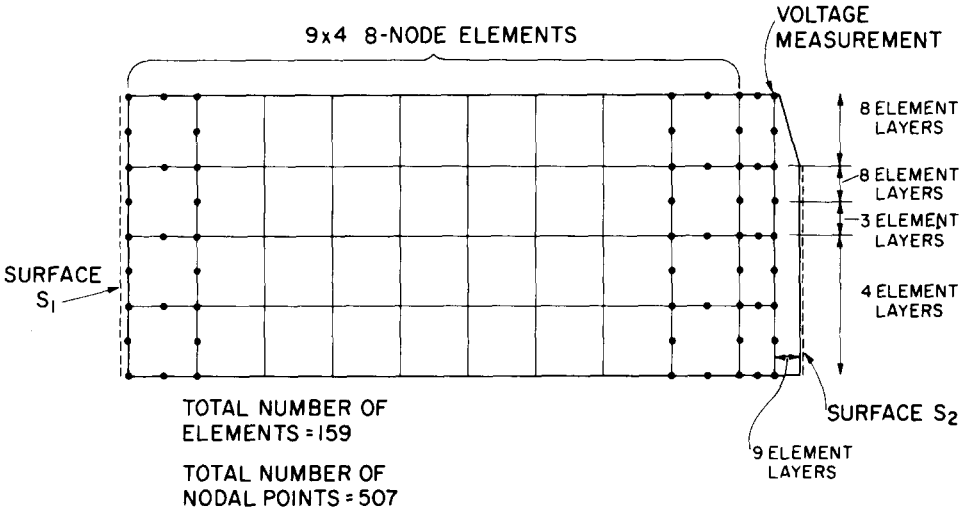

Fig. 2. Finite element idealization of SEN specimen.

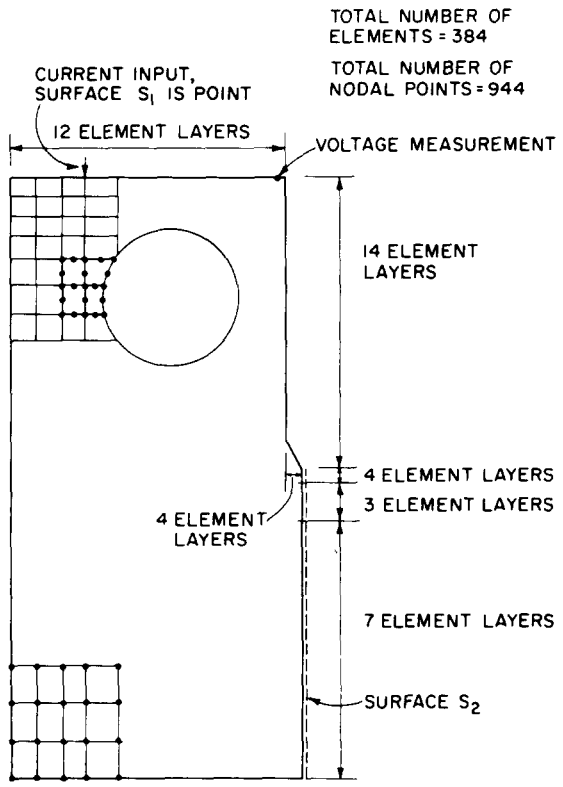

Fig. 3. Finite element idealization of CT specimen.

number-nodes isoparametric elements in which for an element [20],

$$x = \sum_{i=1}^{N} h_i x_i; \quad y = \sum_{i=1}^{N} h_i y_i \tag{5}$$

and

$$\phi = \sum_{i=1}^{N} h_i \phi_i \tag{6}$$

where the h_i are the finite element interpolation functions, x_i, y_i, and ϕ_i are the finite element nodal point coordinates and electric potential of node i, and N is the number of nodes of the element considered. It may be noted that using isoparametric elements in the analysis curved boundaries can directly be approximated. Substituting from Eqns. (5) and (6) for all elements into (2) and invoking the stationarity condition in (4), the governing equations for the electric nodal point potentials, $\boldsymbol{\phi}$, are obtained

$$\boldsymbol{K\phi} = \boldsymbol{Q} \tag{7}$$

where $\boldsymbol{K}$ is the system conductivity matrix, $\boldsymbol{\phi}$ is a vector listing the unknown nodal point potentials and $\boldsymbol{Q}$ is a forcing vector resulting from the boundary current input.

The calibration of the change in the potential as a function of crack depth can now be obtained by resolving (7) for different crack depths; i.e. solving (7) for different surface areas S_2, but keeping the current input constant on surface area S_1.

Since only the boundary conditions are changing on surface area S_2, an incremental solution, in which the conductivity matrix $\boldsymbol{K}$ in (7) (except for the boundary modes) is calculated and factorized only once, is very effective [19, 20].

In the finite element solutions obtained in this study, the computer program ADINAT was employed [20]. Figures 2 and 3 show the finite element idealizations used. A relatively large number of elements were employed to model the material around the notches with the aim to obtain accurate analysis results for short crack lengths.

3. Results

Figures 4–6 show the calibration curves derived numerically in this study, compared with the experimental and theoretical predictions of others [15, 21, 23]. In the analysis of the SEN specimen (Figs. 4 and 5), a theoretical solution from conformal mapping is available [15] and it is observed that the finite element prediction is very close to this solution for shorter crack lengths (Fig. 4). Over a larger range of a/W (Fig. 5), the finite element solution is very similar to experimental [23], electrical analog and conformal mapping [15] solutions, although the capacity of our solution deteriorates somewhat for $a/W > 0.5$, because of the relatively coarse finite element mesh employed away from the notch.

Calibration results for the CT specimen are shown in Fig. 6. Since a theoretical solution does not exist for this specimen, finite element predictions are compared only to experimental results [21, 23]. It is noted that the finite element solution lies consistently below the experimentally obtained non-dimensionalized voltage values, and that the difference grows with increasing crack lengths. The explanation of this discrepancy is not certain at this time, but is probably a function of the effect of crack width on potential. McIntyre and Priest [22] have shown that the potential drop across a flaw increases with the width of the flaw, particularly for longer crack lengths, as is the case for the CT specimen. Since experimental calibrations were obtained with machine slots of width 0.25 mm, whereas the finite element solution considers cracks

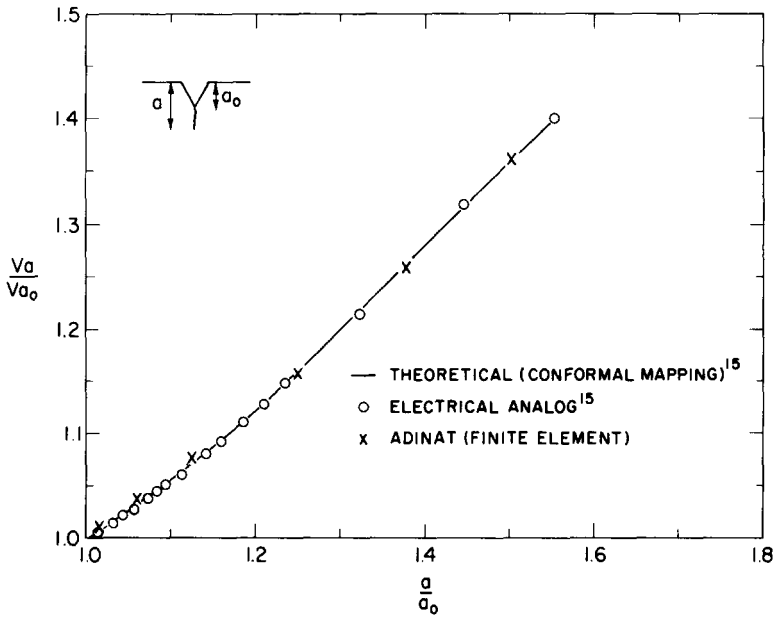

Fig. 4. Calibration curve of SEN specimen at small crack lengths.

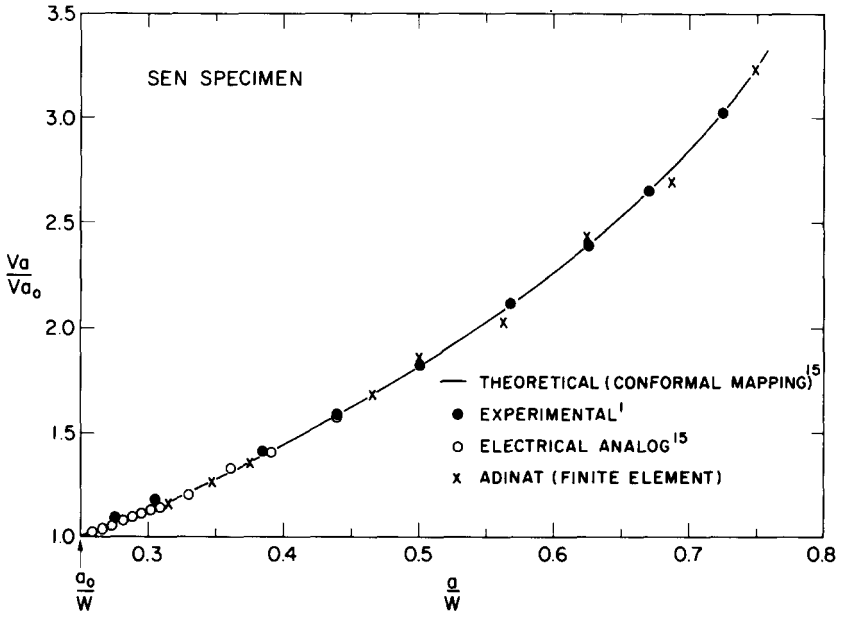

Fig. 5. Calibration curve of SEN specimen for $0.25 < a/W < 0.75$.

of infinitely small width, this effect could possibly give rise to small differences in the two solutions.

4. Discussion

The numerical results derived in this paper indicate that finite element methods provide a quick, accurate and relatively inexpensive way of obtaining theoretical calibrations for various test piece geometries to be used with the electrical potential

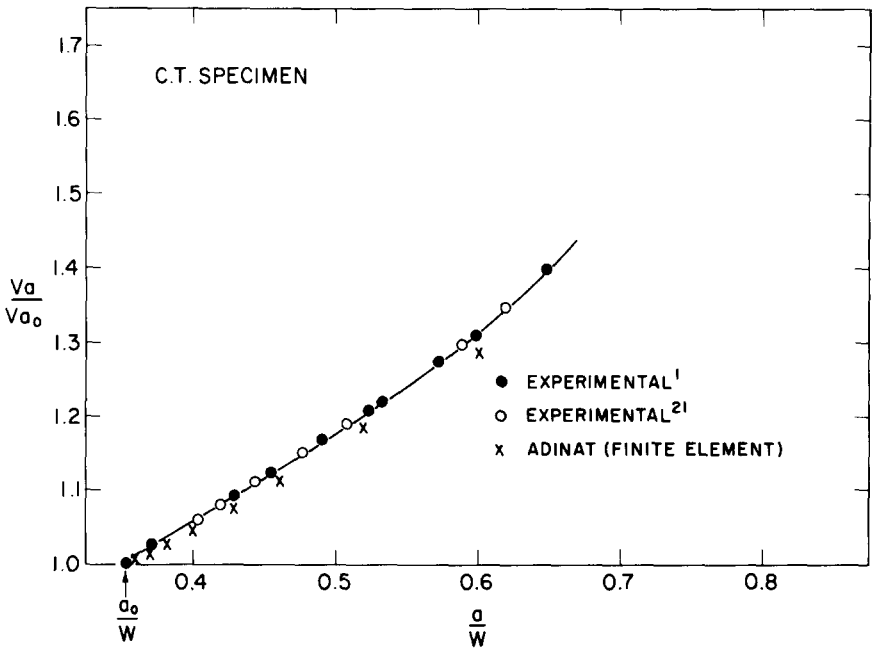

Fig. 6. Calibration curve of CT specimen.

crack-monitoring system. For the more complex test piece geometries, i.e. the CT specimen, numerical procedures provide the only convenient method of obtaining such theoretical calibrations. The cost of these analyses is relatively small compared to the man-hours required to obtain a similar experimental calibration. Our solutions were obtained with little experimentation on the nature of the finite element mesh. Optimizing this mesh would probably provide greater accuracy, particularly at longer crack lengths, and also lead to reductions in cost.

Finite element calibrations, moreover, have the important potential of providing a means to estimate errors due to changes in electrical resistance from crack tip plasticity in a test piece under load. Whether tests are being performed under fatigue, creep, sustained load or rising load situations, material at the crack tip will become plastically deformed, and this effect will locally change the electrical resistivity and hence alter the potential (V_a) measured across the crack. Although the error, when using the electrical potential technique, is small compared to the effect of crack tip plasticity on measurements of crack opening displacement (an alternative method of monitoring the initiation and growth of cracks), the plasticity effect can nevertheless mask the indication of a potential change due to crack initiation in, say, elastic–plastic fracture toughness tests [23] (i.e. J_{Ic} tests). In view of the pressing need for an unambiguous method of detecting crack initiation for single specimen determinations of J_{Ic}, instead of employing expensive multi-specimen R-curve procedures [9], electrical potential calibrations, where the potential change due to plasticity can be differentiated from the potential change due to cracking, would be highly desirable.

This may be achieved for a given material by initially measuring experimentally the change in electrical resistivity with deformation in unnotched tensile specimens. Finite element procedures could then be utilized to estimate the extent of crack tip plasticity* in fracture test pieces, from flow stress and applied load or stress intensity data, to allow a determination of the additional variation in electrical potential from

* In the simplest case of small-scale yielding, this would simply be a measure of the plastic zone size.

the region of plasticity. Comparison of these solutions (i.e. potential vs. crack length under elastic–plastic conditions) with the current elastic solutions (which do not account for yielding) would permit separation of the potential changes due to crack extension and due to crack tip plasticity. Future work will be directed along these lines to provide a means of detecting crack initiation and monitoring crack growth in test pieces undergoing extensive yielding for materials of varying electrical resistivity.

Conclusions

Finite elements analysis procedures have been utilized to provide accurate and relatively inexpensive theoretical calibrations for the electrical potential crack-monitoring system as applied to single-edge-notch (SEN) and compact tension (CT) fracture specimens. The solutions developed compare closely with experimental, electrical analog and analytical (conformal mapping) calibrations obtained for the same test pieces, particularly at short crack lengths.

Acknowledgements

The authors wish to thank N. Sivanera for computational assistance and Professor F.A. McClintock for his many helpful suggestions.

REFERENCES

[1] R.O. Ritchie, G.G. Garrett and J.F. Knott, *International Journal of Fracture Mechanics*, 7 (1971) RCR 462.
[2] A. Trost, *Metallwirtsch.*, 23 (1944) 308.
[3] G. Gille, *Maschinenschaden*, 29 (1956) 123.
[4] R.O. Ritchie and J.F. Knott, *Acta Metallurgica*, 21 (1973) 639.
[5] W.J. Barnett and A.R. Troiano, *Journal of Metals*, 9 (1957) 486.
[6] P. McIntyre, Proceedings British Steel Conference on Mechanics and Mechanisms of Crack Growth, Cambridge ed. M.J. May (April 1973) 121.
[7] J.R. Haigh, R.P. Skelton and C.E. Richards, Materials Science and Engineering, 26 (1976) 167.
[8] J.M. Lowes and G.D. Fearnehough, *Engineering Fracture Mechanics*, 3 (1971) 103.
[9] J.D. Landes and J.A. Begley, Westinghouse Scientific Laboratories, Paper 76-IE7-JINTF-P3, (May 1976).
[10] A.J. Carlsson, *Transactions Royal Institute, Stockholm*, Sweden, No. 189 (1962).
[11] K.D. Unangst, T.T. Shih and R.P. Wei, *Engineering Fracture Mechanics*, 9 (1977) 725.
[12] R.O. Ritchie and V.A. Chang, unpublished research, Rockwell International Science Center (July 1977).
[13] H.H. Johnson, *Materials Research and Standards*, 5 (1965) 442.
[14] Che-Yu Li and R.P. Wei, *ibid*, 6 (1966) 392.
[15] G. Clark and J.F. Knott, *Journal of the Mechanics and Physics of Solids*, 23 (1975) 265.
[16] A.A. Anctil, E.B. Kula and E. DiCesare, *Proceedings of American Society Testing Materials*, 63 (1963) 799.
[17] D.M. Gilbey and S. Pearson, Royal Aircraft Establishment Technical Report No. 66402, Farnborough, England (Dec. 1966).
[18] O.E. Zienkiewicz, in *The Finite Element Method in Engineering Science*, McGraw-Hill Book Co. (1971).
[19] K.J. Bathe and E.L. Wilson, in *Numerical Methods in Finite Element Analysis*, Prentice-Hall (1976).
[20] K.J. Bathe, "ADINAT—A Finite Element Program for Automatic Dynamic Incremental Nonlinear Analysis of Temperatures", Acoustics and Vibration Laboratory Report 82448-5, MIT (1977).
[21] G.G. Garrett, Ph.D. Thesis, University of Cambridge (July 1973).
[22] P. McIntyre and A.H. Priest, BISRA Open Report No. MG/54/71, British Steel Corporation, London (1971).
[23] R.O. Ritchie, Department of Metallurgy, University of Cambridge, Internal Report (Jan. 1972).

RÉSUMÉ

Des procédures d'analyse par éléments finis sont utilisées pour fournir la courbe de calibrage théorique dans le cas d'un système d'avertissement de fissuration par potentiel électrique tel que appliqué dans les éprouvettes à entaille simple latérale et dans les éprouvettes de traction compactes utilisées pour l'étude de la rupture. Les résultats sont comparés avec les calibrages existants pour des géométries d'éprouvettes d'essai de ce type, qui dérivent de procédures expérimentales analogiques électriques et analytiques par représentation conforme.